An integrated techno-economic, environmental and social assessment of the solar thermochemical fuel pathway

Christoph Falter*[a], Antonio Valente[b,c,§] , Antoine Habersetzer[a], Diego Iribarren[b], Javier Dufour[b,c]

[a.] *Bauhaus Luftfahrt, Willy-Messerschmitt-Str. 1, 82024 Taufkirchen, Germany.*
[b.] *IMDEA Energy - Systems Analysis Unit, 28935 Móstoles, Spain.*
[c.] *Chemical and Environmental Engineering Group, Rey Juan Carlos University, 28933 Móstoles, Spain*
[§]*Current address: Department of Chemistry and Applied Biosciences, Institute for Chemical and Bioengineering, ETH Zurich, Vladimir-Prelog-Weg 1, 8093 Zurich, Switzerland*

Supplementary Information

Computational model of the thermochemical redox cycle

The computational model used for the calculation of the energy balance of the thermochemical redox reaction is based on the work performed in Falter et al. [1]. The following values[2] are assigned to the parameters to achieve the proposed efficiency of 19% (excluding the energy for vacuum pumping and gas separation).

Table S.1 Parameter values for thermochemical redox cycle.

Parameter	Value	Unit
Concentration ratio	5000	-
Oxidation temperature	1000	K
Reduction temperature	1900	K
Efficiency gas heat recuperation	0.7	-
Efficiency solid heat recuperation	0.7	-
Reduction pressure	1100	Pa
Oxidation pressure	1.013×10^{5}	Pa
Efficiency CO_2 conversion	0.5	-

Optimisation of reactor efficiency with respect to reduction pressure

The reduction pressure of the reactor is varied to maximise energy conversion efficiency (Figure S.1).

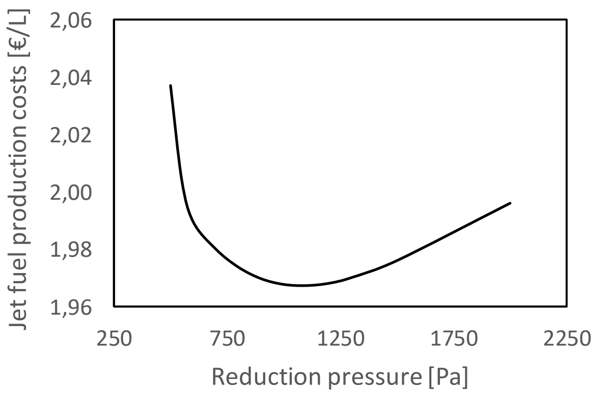

Figure S.1 Optimization of reactor efficiency with respect to reduction pressure.

Additional economic information

Table S.2 Financial assumptions for different countries.

Country	Inflation [%][a]	Debt interest rate [%][b]	Equity interest rate [%][c]	Nominal weighted av. cost of capital [%][d]
Morocco	1.24	5.70	11.78	8.13
USA	1.32	4.05	8.20	5.71
Spain	0.52	2.20	8.88	4.87
Australia	1.96	5.27	7.70	6.24
Chile	3.32	4.58	10.78	7.06
South Africa	5.62	10.39	17.12	13.08

[a] The interest rates are the average of the years 2013-2017 and are taken from the World Bank[3].

[b] The debt interest rates are bank prime lending rates from the IMF[4].

[c] The equity interest rates are the sum of government bond yields and equity risk premiums, taken from [5,6] and Damodoran[7].

[d] The nominal weighted average cost of capital is derived from the debt (d) and equity (e) interest rates as follows: $WACC(nom)=0.6\times d+0.4\times e$.

Table S.3 Energy requirements, efficiencies, and costs of process steps in the baseline case. Where not otherwise specified, the values are based on own computations.

Process step	Value	Unit	Source
H_2O/CO_2 capture from air			
Electricity	300	kWh/t	8
Heat	1500	kWh/t	8
Investment costs	350	€/(t y)	
O&M costs	40	€/t	
H_2O storage[a]	7.73×10^6	€	9
CO_2 storage (compressors)[a]	12.6×10^6	€	10
CO_2 storage (tanks)[a]	28.9×10^6	€	11
Concentration of sunlight			
Optical efficiency	51.6%	-	12
Costs of heliostats	100	€/m^2	
Costs of tower	20	€/kW$_{th}$	13
Thermochemistry			
Costs of reactors	12	€/kW$_{th}$	
Jet vacuum pumps[a,c] (inv. costs)	58.6×10^6	€	14
Ceria	5	€/kg	
Syngas storage[a]			
Pressure level	16	bar	
Power level (H_2 compression)	14.5	MW	
Power level (CO compression)	6.50	MW	
Inv. costs (H_2 compression)	9.70×10^6	€	10
Inv. costs (CO compression)	4.44×10^6	€	10
Fischer-Tropsch synthesis			
Pressure level	25	bar	
Investment costs	23000	€/bpd	15
O&M costs	4	€/bbl	15
Hydrocracking[b]			
Heat	5.2	MW	
Electricity	0.9	MW	
Steam reforming[b]			
Heat	39.9	MW	
Electricity	10.0	MW	
CO_2 capture with MEA[a]			
Heat	84.1	MW	
Electricity	0.52	MW	

Water input	1.34	L/FU	
Investment costs	12.9×10^{6}	€	16
Product pipeline[a]			
Investment costs	90	€/m	17
Ship transport			
Unit cost	8×10^{-3}	€/L	18
Labour costs			
Number of managers	5		
Number of engineers	30		
Number of clerks	15		
Number of technicians	100		
Number of workers	246		
Salary of managers	13890	$/y	19
Salary of engineers	7746	$/y	19
Salary of clerks	3869	$/y	19
Salary of technicians	5646	$/y	19
Salary of workers	3839	$/y	19

[a] The associated O&M costs are 5% of the investment costs.

[b] The associated costs are assumed to be included in the cost of FT.

[c] The O&M costs are included in the labour costs.

Table S.4 Cost estimate of solar thermochemical reactors.

Single reactor unit at 50 kW capacity	**Cost [$]**
Shell / pressure vessel	6,500
Piping	1,000
Insulation	15,000
Flange and front	6,500
Window	500
Window Mount	1,000
Active radiation shield	2,500
Mounting/structure	3,000
Misc. hardware	1,000
Equipment: vacs	10,000
Equipment: valves	1,000
Equipment: sensing	2,000
Equipment: control	5,000
Total cost	**55,000**
Unit cost per kW (single reactor)	1100 $
Unit cost per kW (at GW-scale with scaling factor 0.6)	12 €

Additional information regarding the social assessment

Table S.5 Specific social risk levels for the country-specific sectors involved in the baseline case.

Country	PSILCA sector	Child labour	Forced labour	Health expenditure	Used for
Morocco (MA)	Electricity, gas and water supply	Low	Low	High	Working hours at the fuel plant
Morocco (MA)	Maintenance and repair	Low	Low	High	O&M (solar field, CO_2 and H_2O)
Morocco (MA)	Construction	Low	Low	High	Buildings
Spain (ES)	Electrical machineries and apparatus	No	Very low	Low	Heliostats
Spain (ES)	Electric machinery and material	No	Very low	Low	Cables
Spain (ES)	Construction	No	Very low	Low	Pedestal
Spain (ES)	Other services and activities	No	Very low	Low	Overhead
Spain (ES)	Manufacture of fabricated metal products	No	Very low	Low	Gear drive
Spain (ES)	Manufacture of glass and glass products	No	Very low	Low	Mirrors
China (CN)	Metal products	High	Very low	Medium	Pipelines
China (CN)	Chemicals for special usages	High	Very low	Medium	Ceria
Czech Republic (CZ)	Machinery and equipment	No	Low	Medium	Compressors
India (IN)	Manufacture of fabricated metal products	Very low	High	High	Gas separator
USA	Power boilers and heat exchangers	No	Very low	Medium	Reactors
France (FR)	Machinery and equipment	No	Very low	Low	O&M (syngas storage, valves, pump); vacuum pumps
Portugal (PT)	Manufacture of basic metals	Low	Very low	Medium	Steel (mix)
Turkey (TR)	Manufacture of basic metals	Low	Low	Medium	Steel (mix)
USA	Other industrial machinery manufacturing	No	Very low	Very low	CO_2 capture
China (CN)	Other general industrial machinery	High	Very low	Medium	Valves, checks
Germany (DE)	Basic ferrous metals	No	Very low	Low	Steel (mix)
France (FR)	Manufacture of basic metals	No	Very low	Low	Steel (mix)
Italy (IT)	Manufacture of basic metals	No	Very low	Medium	Steel (mix)
Germany (DE)	Communication and electronic equipment	No	Very low	Low	Motor
China (CN)	Non-metal minerals and other mining	High	Very low	Medium	Cerium mining

Table S.6 Social life-cycle profile of the jet fuel when considering alternative locations of the solar jet fuel plant (values in mrh per litre of jet fuel).

Country	Child labour	Forced labour	Health expenditure
Morocco (baseline)	1.08×10^{-1}	1.30×10^{-2}	3.03×10^{9}
Spain	1.27×10^{-1}	5.49×10^{-4}	8.92×10^{-2}
USA	1.39×10^{-1}	5.48×10^{-4}	1.10×10^{-1}
Australia	2.52×10^{-1}	4.59×10^{-4}	9.95×10^{-2}
Chile	3.22×10^{-1}	8.58×10^{-4}	2.43×10^{-1}
South Africa	6.17	6.42×10^{-3}	2.42×10^{-1}

Social inventory data schemes for alternative plant locations

Australia

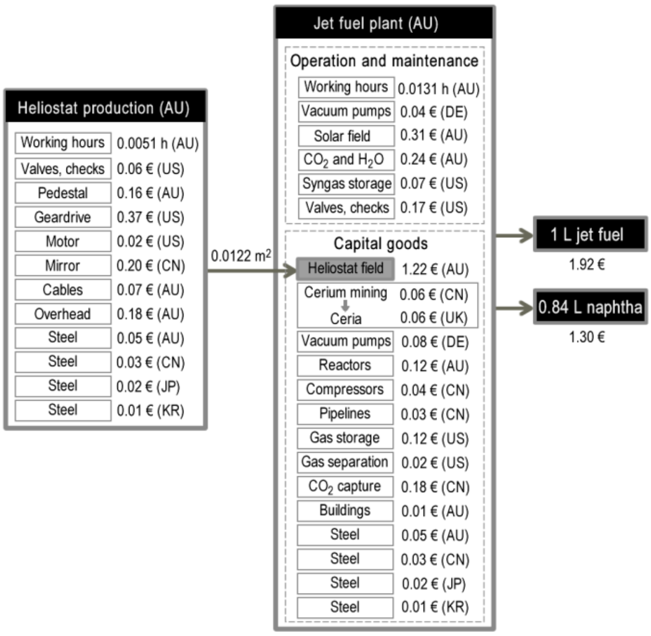

Figure S.2 Techno-economic flows and source countries for the SLCA of the case of Australia.

Spain

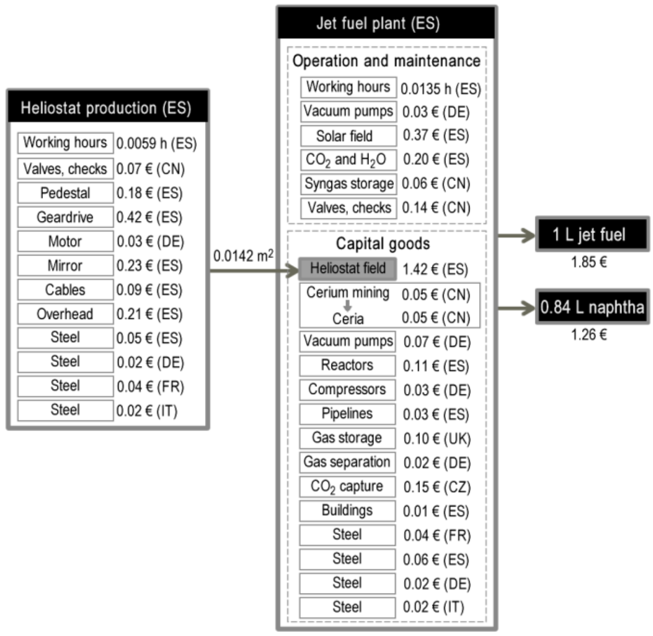

Figure S.4 Techno-economic flows and source countries for the SLCA of the case of Spain.

Chile

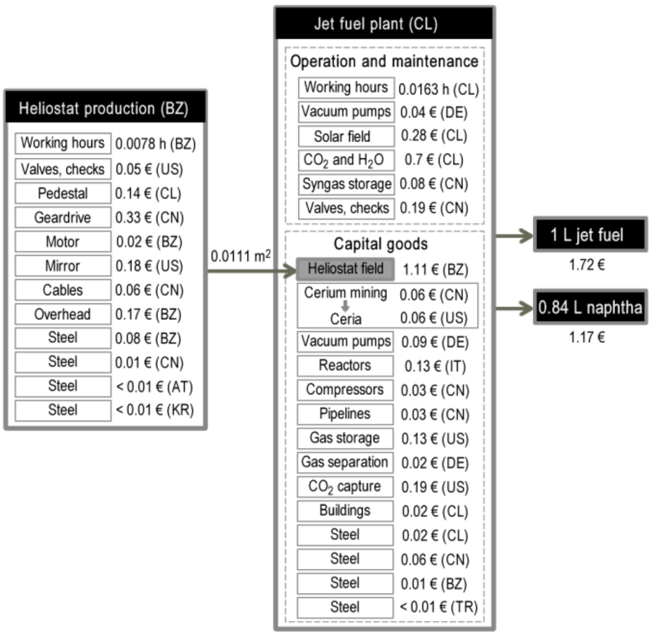

Figure S.3 Techno-economic flows and source countries for the SLCA of the case of Chile.

USA

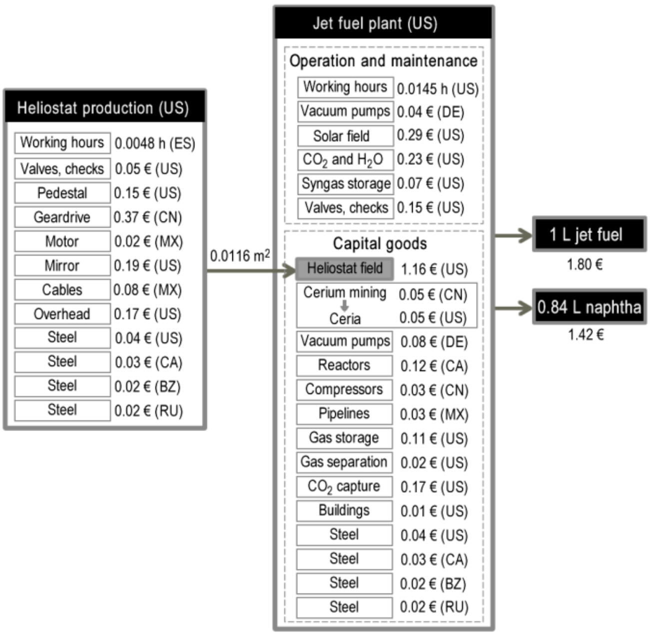

Figure S.5 Techno-economic flows and source countries for the SLCA of the case of USA.

South Africa

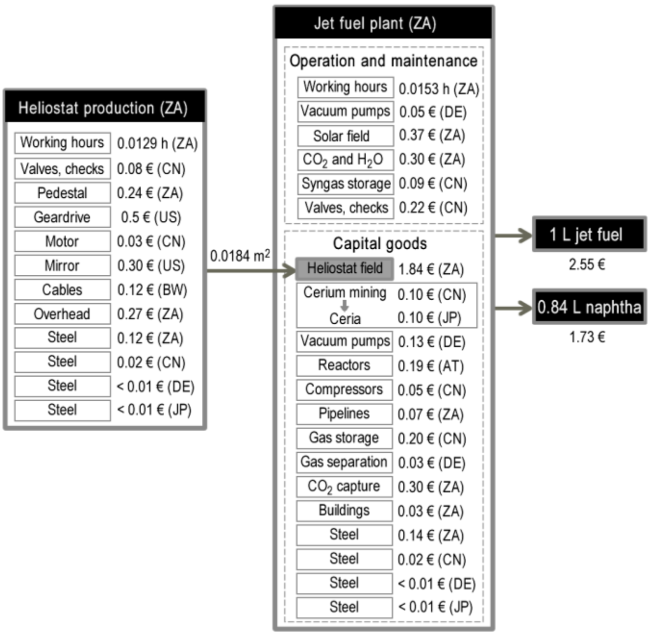

Figure S.6 Techno-economic flows and source countries for the SLCA of the case of South Africa.

Aspen model for the simulation of syngas conversion

In the following, the computational Aspen Plus model for the derivation of mass and energy balances of the syngas-to-fuel conversion is shown.

Process diagram for whole plant

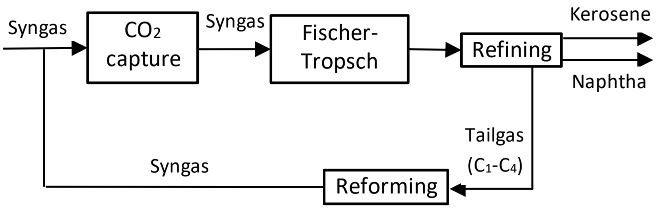

Figure S.7 Process model of syngas-to-fuels conversion. CO_2 capture reduces the share of CO_2 in the gas mixture (H_2+CO+CO_2). The Fischer-Tropsch synthesis produces hydrocarbons of different chain lengths in the gaseous, liquid, and waxy regime, where the gaseous fraction is steam reformed back into syngas.

CO_2 separation with monoethanolamine (MEA)

As only half of the CO_2 entering the solar thermochemical reactor is converted into CO, CO_2 has to be separated from the syngas to reduce its partial pressure in the FT reactor. This is done via chemical absorption with monoethanolamine.

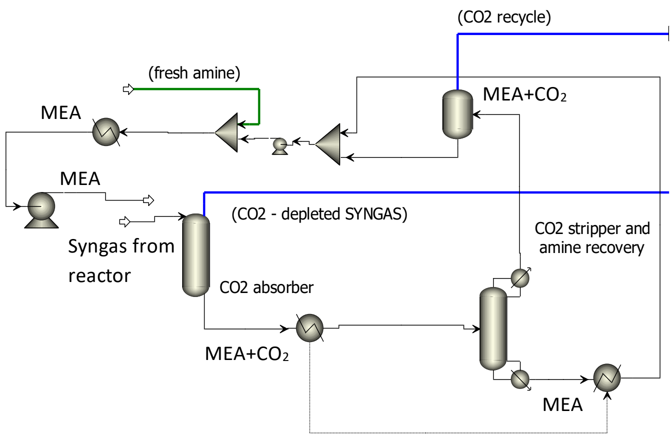

Figure S.8 Process model for CO_2 capture with MEA.

Fischer-Tropsch conversion

The syngas, having been cleaned from CO_2, is sent to the Fischer-Tropsch reactor (25 bar; H_2/CO feed ratio of 1.7), where hydrocarbon chains of different length are assembled. The light fractions are subsequently separated via flash distillation.
The model behind this step is based on the kinetic model in Visconti and Mascellaro 2013 [20].

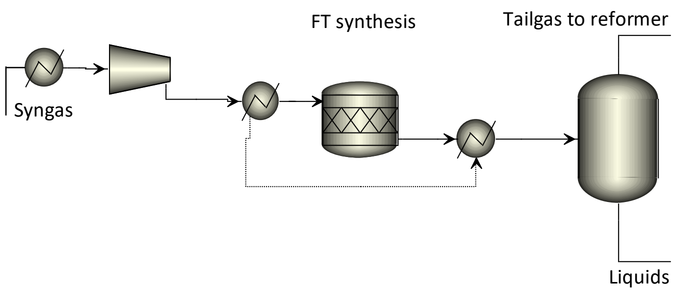

Figure S.9 Process model for Fischer-Tropsch conversion. The syngas entering the compression has been subject to CO2 removal. The FT synthesis operates at a pressure of 25 bar and a temperature of about 220°C. The tailgas is composed of the gaseous fraction of hydrocarbons produced.

Refining

The FT synthesis is carried out at low temperature using a Co-based catalyst to create long-chained hydrocarbons. To receive the desired regime of C_8-C_{16}, the hydrocarbons need to be cut to shorter lengths via hydrocracking. At first, water is separated from the FT liquids, which are then sent to a first flash separator to remove light fractions. In the hydrocracker, the long-chained hydrocarbons are cut to shorter lengths with hydrogen at elevated pressure and temperature. Further separation steps separate the jet fuel from naphtha and tail gas.

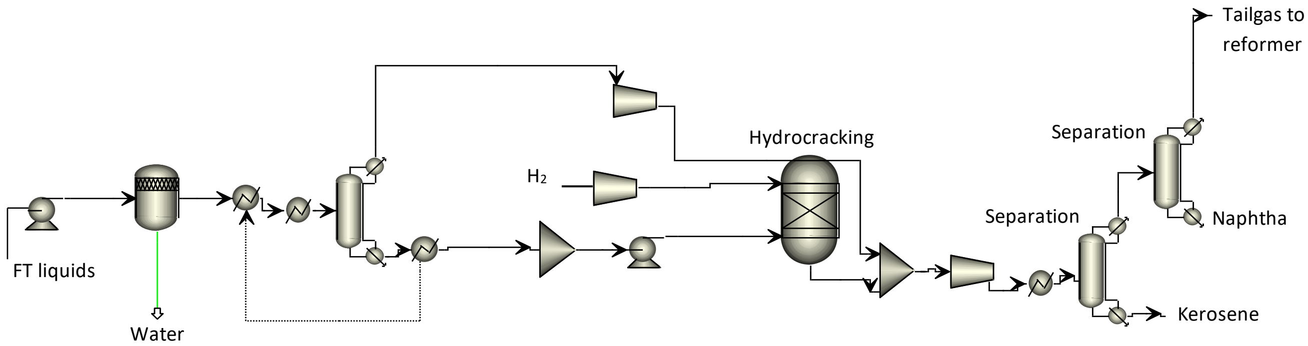

Figure S.10 Process model for the refining of FT liquids. The liquids are composed of hydrocarbons with a chain length of >C_5 and water, which is removed. A flash distillation separates hydrocarbons into different chain lengths, where the longer fractions are cracked into shorter lengths with H_2. The resulting liquid mixture is then separated into its kerosene and naphtha fractions, and a gaseous fraction that returns to the steam reformer.

Reforming

The gaseous fraction from the hydrocracker is reformed with steam to syngas, which is then fed back into the process to increase the conversion of syngas to fuels. In the steam reformer, syngas is produced from the tail gas of the hydrocracker and water. The syngas is then cleaned and compressed to be fed back into the system before the FT synthesis.

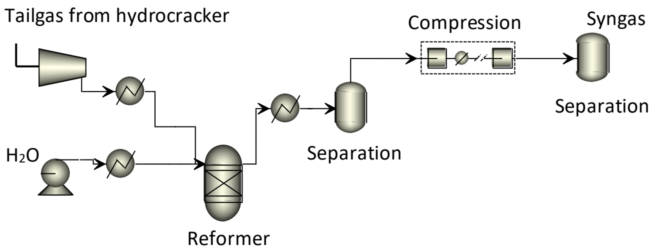

Figure S.11 Process model for steam reforming of light hydrocarbons.

Additional environmental life-cycle indicators

Table S.7 presents an additional set of environmental life-cycle indicators that complement the assessment of the environmental performance of the fuel pathway. The chosen method is ReCiPe 2016.

Table S.7 Additional environmental life-cycle indicators.

Indicator	Solar fuel	Conv. Fuel	Unit
Stratospheric ozone depletion	7.23×10^{-7}	1.28×10^{-6}	kg CFC-11 eq.
Fine particulate matter formation	4.47×10^{-3}	2.25×10^{-3}	kg PM 2.5 eq.
Terrestrial acidification	1.15×10^{-2}	6.43×10^{-3}	kg SO_2 eq.
Fossil depletion	0.399	1.74	kg oil eq.
Fresh water consumption	2.31×10^{-2}	8.50×10^{-3}	m^3
Human toxicity, cancer	1.31×10^{-6}	5.40×10^{-8}	DALY
Human toxicity, non-cancer	1.66×10^{-6}	1.16×10^{-7}	DALY
Climate change human Health, default, excl. biogenic carbon	-3.04×10^{-6}	6.89×10^{-7}	DALY

References

1 C. P. Falter and R. Pitz-Paal, *Sol. Energy*, 2017, **144**, 569–579.
2 C. Falter, A. Sizmann and R. Pitz-Paal, in *AIP Conference Proceedings*, 2017, vol. 1850.
3 Worldbank, Inflation, consumer prices (annual %).
4 IMF, Lending rates, Percent per annum.
5 Trading Economics, Government Bond yields.
6 World Government Bonds, 10 Year Bond Yields, http://www.worldgovernmentbonds.com/, (accessed 8 October 2019).
7 A. Damodoran, Estimated Country Risk Premiums.
8 Climeworks LLC., CO2 air capture demonstration plant, http://www.climeworks.com/co2-capture-plants.html, (accessed 1 June 2014).
9 G. Wernet, C. Bauer, B. Steubing, J. Reinhard and B. Moreno-Ruiz, E., Weidema, *Int. J. Life Cycle Assess.*, 2016, **[online] 2**, 1218–1230.
10 S. T. McCoy, *Diss. Carnegie Mellon Univ.*
11 B. D. James, C. Houchins, J. M. Huya-Kouadio and D. A. Desantis, 2016, 1–54.
12 Sargent&Lundy, *Assessment of Parabolic Trough and Power Tower Solar Technology; SL-5641*, Chicago, IL, USA, 2003.
13 T. R. Mancini, J. A. Gary, G. J. Kolb and C. K. Ho, *Power Tower Technology Roadmap and Cost Reduction Plan.*, Albuquerque, NM, and Livermore, CA (United States), 2011.
14 S. Brendelberger, H. von Storch, B. Bulfin and C. Sattler, *Sol. Energy*, 2017, **141**, 91–102.
15 Velocys, 2013.
16 J. Kim, T. a. Johnson, J. E. Miller, E. B. Stechel and C. T. Maravelias, *Energy Environ. Sci.*, 2012, **5**, 8417.
17 M. S. Peters, K. D. Timmerhaus and R. E. West, *Plant Design and Economics for Chemical Engineers*, 2003.
18 US Department of Transportation, Average Freight Revenue, https://www.bts.gov/archive/publications/national_transportation_statistics/2000/3-17, (accessed 18 January 2019).
19 ILO, Mean nominal monthly earnings of employees by sex and occupation-- Harmonized series.
20 C. G. Visconti and M. Mascellaro, *Catal. Today*, 2013, **214**, 61–73.